Article:

Li, W, Zhao, S, Li, K orcid.org/0000-0001-6657-0522 et al. (3 more authors) (2023) GSOANR-based multi-objective train trajectory optimization. International Journal of Rail Transportation. ISSN 2324-8378

https://doi.org/10.1080/23248378.2023.2194684

GSOANR based multi-objective train trajectory optimization

Wei Li[a], Sizhe Zhao[a], Kang Li[b], Yi Xing[a,c], Qian Li[a], Wenhua Yao[a,c]

[a] School of Traffic & Transportation, Central South University, Changsha, Hunan, China; [b] School of Electronic and Electrical Engineering, University of Leeds, Leeds, West Yorkshire, England; [c] CRSC Research & Design Institute Group Co., Ltd. Beijing, China

Abstract: Railway transport is an important transportation mode in China, UK and worldwide. It is expected to play an even more important role in transportation decarbonization in shifting more passenger trips and freight transportations to railway. It is strategically important to reduce the energy consumption and improve the overall energy efficiency of the railway systems. The introduction of automatic train operation (ATO) systems in electrified railway systems makes it possible to achieve energy consumption reduction while satisfying other railway operation criterions such as the need for passenger comfort, train punctuality and safety. Although energy saving of railway systems has attracted substantial interests in recent years, the ATO system are not environmentally-friendly as expected and there is a lack of a set of energy saving performance measures for railway system planning and operation. In this paper, the features of ATO systems are incorporated into the problem formulation, and a modified GSO algorithm with adaptive neighborhood range (namely the GSOANR algorithm) is proposed as the solver of the problem. The proposed method is applied to the trajectory planning of a 58km long route between Heishan North Station and Fuxin Station of the Beijing-Shenzhen Line in China, and the results confirm that the train operation trajectory generated by the GSOANR algorithm-based optimization method can reduce the electrical energy consumption by about 5.6% compared with the results generated by the standard GSO algorithms, confirming the efficacy of the proposed energy-saving measures and the effectiveness of the novel optimization method, and the referential significance for the study of the train trajectory optimization.

Keywords: Train trajectory optimization; Energy-efficient train operation; Energy Saving Measures; Multi-objective optimization; Modified GSO algorithm

1. Introduction

The railway system is a large energy consumer in many countries and regions. For example, Network Rail is the single biggest electricity user in the UK, consuming over 4 TWh per year, accounting for over 1% of the total national electricity demand, spending over £300 million on electricity with £250 million on the rail traction alone. Likewise, the railway consumes over 60 TWh electricity per year in China, around 60 TWh in Europe, and 5.8 TWh in Japan. In China, the high-speed rail (HSR) is the world's longest with the total length reaching 37,900 kilometers by the end of 2020, which accounts for over 70% of the global HSR networks. The fast-growing pace of electrified railway systems and HSR has called for energy savings and efficiency improvement along with the transition to transportation decarbonization. Considering that the majority of energy consumption in railway comes from the traction, the operation mode optimization and energy storage of the trains becomes the key for energy reduction and efficiency improvement, and has been intensively researched in recent years [1-5].

The existing approaches for train trajectory optimization can be broadly categorized into two groups, the analytic methods and meta-heuristic methods. Albrecht et al. developed a formulation to model energy consumption for train control and demonstrated the existence of optimal control and switching points [6-7]. Bai et al. studied the real-time optimization problem of train operation and developed a fuzzy predictive control method to reduce the energy consumption of the train operation while meeting the speed limit [8]. Then Zhou et al. proposed a macro and micro computation framework of train operation diagrams and the optimal speed/acceleration curve, which was further tested to confirm the efficiency on the Beijing-Shanghai line [9]. Based on the research of the ATO control strategy, Liu et al. proposed a single-vehicle optimization model which can effectively optimize the train operation trajectory [10]. In 2019, Zhang et al. established an energy-efficient operation model to reduce the energy consumption based on the Q-learning algorithm [11]. On the basis of the former studies, some scholars have tried to combine the intelligent algorithms with the train ATO control strategy, bringing new ideas to solve the problem of energy-saving train operation optimization [12-14].

The analytic methods such as the dynamic programming and other approaches mentioned earlier suffer from issues such as complicated modeling, performance being dependent on the parameter settings of the model. While meta-heuristic approaches can adapt well to complex and nonlinear problems, and to use meta-heuristic approaches for the train operation optimization is becoming more and more popular.

This paper is dedicated to solving the problem of optimizing energy-efficient train operations due to the development of ATO systems. A modified glowworm swarm optimization algorithm, namely GSOANR, is proposed and the effectiveness of the method is investigated through extensive simulation studies. The main contribution of this paper is the raise of the GSOANR algorithm and the definition of the working conditions of the train operation process. This paper is dedicated to make an attempt to solve the train operation trajectory optimization problem and to contribute to the development of energy-efficient railway transport systems.

2. Energy-efficient operation system method and basic optimization strategy

2.1. Train operation process modelling and analysis

Theoretically, there exist an infinite number of operating trajectories satisfying a given train operating time requirement, subject to the line conditions and speed limits, etc. It was reported that under the same conditions of line speed, gradient, and other related factors, the energy consumptions with different trajectories can differ by 30% [15]. The trajectories are generated by the optimization layer of the on-board ATO system in form of the train operation curve, and the relevant on-board equipment is illustrated in **Figure 1**.

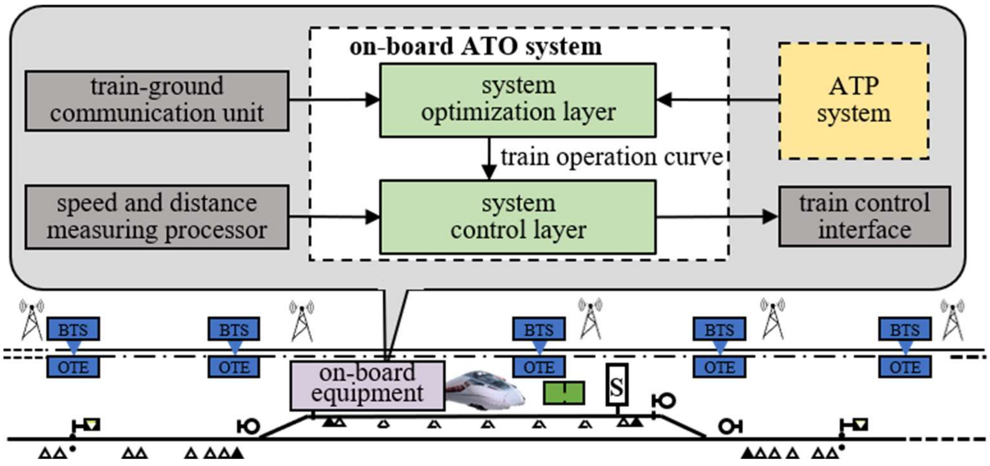

Figure 1. Operating principle of the onboard ATO system in high-speed trains.

The onboard ATO system introduced in electrified trains, in particular for high-speed trains can often be divided into two main layers[16]. As presented in the system optimization layer is mainly responsible for generating an operation trajectory, which should take the given line and operation constraints into consideration, and pass it to the control layer; the function of the control layer is mainly comparing the real-time speed of the train with the targeted speed received from the optimization layer, then the control unit outputs control commands in order to achieve the targeted traction operation.

In this way, optimizing the operation trajectory of the high-speed trains while meeting various constraints can achieve energy saving in the traction system. To optimize the train operation for energy-saving, this section analyzes the train operation process at first.

During the process of running, a train is powered by the traction system and its movement has to overcome a variety of resistances, hence requiring energy consumption. The kinetic equation of a train is composed of the longitudinal forces of the train [17-18], the combined force of the train varies by location, and can be described as six driving conditions. When the train stars to accelerate, the condition of the train is constant-torque traction mode (CTTM). Then the train runs on the constant-power traction mode (CPTM) and cruising mode (CRM) on the line. One upon the train stops applying the traction force, it will be in coasting mode (COM). Finally, the train will switch to electric braking mode (EBM) and stopping mode (SM) to stop at the station. There is an ideal train running speed trajectory showed in **Figure 2**. In practical operations, the train uses electric brakes to reduce the operating speed, and only air brake is only used for emergency brake and entering stations. Hence the stopping mode which uses pneumatic brake only appears at the end of the curve.

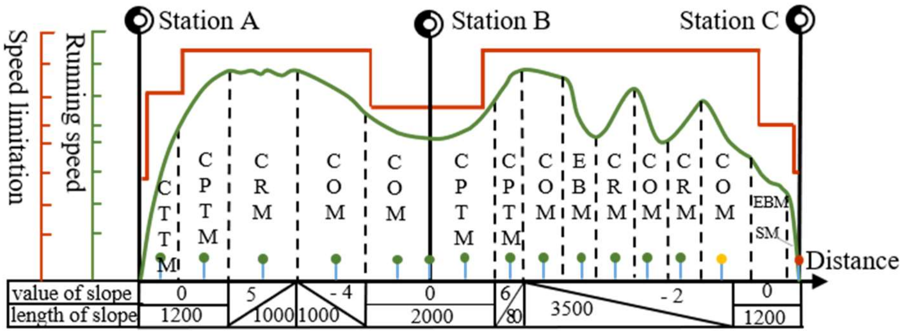

Figure 2. Description of the running process.

Summarily, in practical train operation, the adjustment of train operation trajectory usually follows the six operation modes. The movement of the train from the initial position to the target position therefore can be formulated as a series of traction control sequences, each being operated for a certain length of distance so that a complete set of train maneuvering strategies can be determined and optimized to achieve energy saving.

2.2. Performance indicators for operating trajectory optimization

Generating a train speed trajectory, which not only meets the energy-saving target but also satisfies all required constraints, is the most important purpose of the operation optimization. The train operation status can be affected by many factors including the line conditions, control signals, train characteristics, and the comfort requirements of the passengers while traveling, so it is necessary to define the train operation performance measures first, and then the corresponding energy consumption optimization model can be derived.

Table 1. Symbols.

Symbol	Description
T	The journey time
A	Auxiliary energy efficiency parameter
E	Energy consumption indicators
f_t、b_b	The traction force and the braking force, respectively
M	Mass of the train
μ_f、μ_b	Electrical energy conversion efficiency in motoring mode and braking mode, respectively
s_0、s_n	The beginning and ending of the interval of the corresponding mode
P_t	The ravel time index penalty function
P_s	The stopping position index penalty function
$\bar{a}$	The average acceleration valve in time interval
$f_t(v)$	Unit traction force
$w(s)$	Unit resistance force
$b_b(v)$	Unit braking force
$x_{ij}(n)$	The jth value of the ith individual firefly

In order to facilitate the analysis of the train operation process, the following assumptions are made for the research questions:

(1 The utilization of regenerative feedback energy is not considered;

(2 The traction force and braking force of the train are continuous, and the train can run at a constant speed;

(3 Since the emergency braking conditions are generally not used in the normal operation of the train, the train braking conditions in this paper are limited to the common braking conditions;

(4 The energy consumption of the auxiliary systems, such as lighting, air conditioning and fans, is only related to the running time and has nothing to do with the operating conditions of the train.

Energy consumption measure. The energy consumed by high-speed trains includes the traction energy and the non-traction energy which is caused by the air conditions and the lights on the train. The former consumption is equal to the integral of the traction force against the distance, and the later one is often proportional to the journey time T with the auxiliary energy efficiency parameter A. The energy consumption indicators E during the operation is shown in **Equation (1)** [19-21].

$$E = \frac{1}{\mu_f}\int_{s_0}^{s_n} M \cdot g \cdot f_t(v)\mathrm{d}s + A \cdot \frac{T}{3600} - \mu_b \int_{s_0}^{s_n} M \cdot g \cdot b_b(v)\mathrm{d}s \tag{1}$$

Travel time and stopping position measure. When the trains run according to a pre-assigned running plan in the practical applications, the travel time intervals and the stopping position on the stations are often pre-fixed. In calculating the speed trajectory, the travel time index penalty function P_t is presented in **Equation (2)**, and **Equation (4)** defines the stopping position index penalty function P_s, both of them are imposed to avoid unnecessary safety hazards.

$$\Delta t = \left|\sum_{i=1}^{n} t_i - t_p\right| \tag{2}$$

$$P_t = \begin{cases} 1, & \Delta t \le \tau \\ A_{pt}, & \Delta t > \tau \end{cases} \tag{3}$$

$$\Delta s = \left|\sum_{i=1}^{n} s_i - s_p\right| \tag{4}$$

$$P_s = \begin{cases} 1, & \Delta s \le \sigma \\ A_{ps}, & \Delta s > \sigma \end{cases} \tag{5}$$

among them, the deviation value Δt can be expressed as the absolute value of the difference between the driving time in the actual operation time $\sum_{i=1}^{n} t_i$ and the planned time t_p which is pre-fixed in the optimization layer of the ATO system, likewise, Δs is the deviation value of driving distance of the actual operation $\sum_{i=1}^{n} s_i$ from planned distance s_p. The biggest value is 120s of the travel time index and is 0.3m of the stopping position index.

Comfort measure. For passengers, their expectation is a fast, safe and comfortable journey, while intense speed changes during the journey could cause discomfort to passengers. In this paper, except for the energy consumption measure which is the main purpose of the optimization, travel time and stopping position measure which is the basic requirement of the operation, the riding comfort of the passengers is also taken into consideration. The comfort measure can be expressed as the change rate of the acceleration value of the train as follows.

$$G = \bar{a}/\Delta t \tag{6}$$

where, $\bar{a}$ presents the average acceleration valve in time interval Δt.

$$\min J = k_1 \sum_{i=1}^{n} E_i + k_2\left|t_p - \sum_{i=1}^{n} t_i\right| + k_3\left|s_p - \sum_{i=1}^{n} s_i\right| + k_4 max\{G\}$$

$$s.t.\begin{cases} v = \mathrm{d}s/\mathrm{d}t, \\ m \cdot \mathrm{d}v/\mathrm{d}t = f_t(v) - w(s) - b_b(v), \\ 0 \le s_i \le s, i = 1,2,\cdots,n\ \ s_1 = 0, \\ v(s_0) = v(s_n) = 0, v(s_i) \le v_{max}, \\ t(s_0) = 0, t(s_p) \le t_p, 0 \le t(s_i) \le t_p. \end{cases} \tag{7}$$

The objective function $minJ$ is composed of the energy consumption measure, travel time measure, stopping position measure and conform measure, and the importance of each measure is determined by the weight k_i. The dynamics equation of the train is composed of the unit traction $f_t(v)$, unit resistance $w(s)$ and unit braking force $b_b(v)$ of the train. Along the journey, the train starts at position s_0 and stops at position s_n, hence the velocity of the train at the position s_0 and s_n should be 0. v_{max} is the speed limit of subsection s_i, for a traveling train, the speed of the train at position s_i should always below the speed limitation v_{max} and the time consumption should not exceed the planned running time t_p.

2.3. Train operation trajectory optimization

The train operation trajectory optimization problem is actually a maneuvering scheme optimization problem of a train whose departure point is s_0 and the destination is s_i, subjected to the requirement on punctuality, energy saving, and comfort, etc. There are 4 changeover points in **Figure 3** during the process where a train can switch to any driving condition, and the expected costs Q_i of the interval is determined by driving condition, initial velocity and initial location. The evaluation of the resultant trajectory is determined by the performance measure model, and the optimal operation scheme includes the sequence of transition points $\{s\} = [s_1, s_2 \cdots, s_4]$ where the driving conditions changed and the sequence of driving conditions $\{u\} = [u_0, u_1, \cdots, u_4]$.

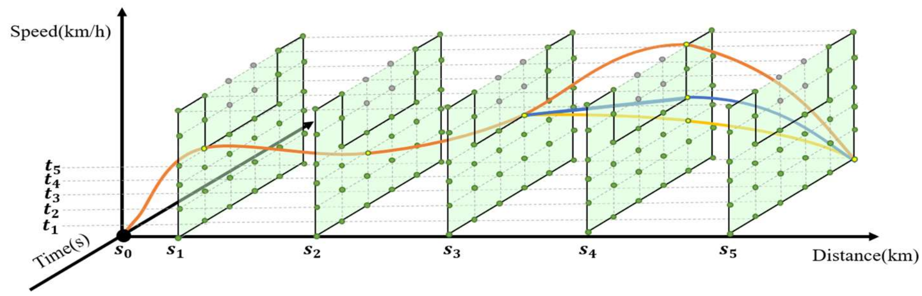

Figure 3. Basic policy of the schematic diagram.

In **Figure 3**, each changeover point s_i is corresponding to a driving condition u_i, having an impact on the operation of the next operation stage and the overall operational performance. The driving condition started at changeover point s_1 determines the speed and location of the train at changeover point s_2. Constrained by the speed limitation and the speed trajectory of the train, the expected cost transferring from one stage to another can be defined as follows, where, u_i is the driving condition in the $[s_i,\ s_{i+1}]$ interval, a_{ui} presents the acceleration under driving condition u_i.

$$\begin{cases} v_0 = 0, \qquad v_1 = \sqrt{2a_{u0} \cdot S_1} \\ v_{i+1} = \sqrt{2a_{ui} \cdot (S_{i+1} - S_i) + v_i^2} \end{cases} \tag{8}$$

Suppose the train adopts the operation condition u_1 at changeover point s_1, then it continues to travel to the changeover point s_2, the expected cost achieved during the interval is defined as Q_1, which is calculated according to **Equation (7)**. The lower the expected cost, the better the resultant solution is, and the state transition at stage i can be described as follows.

$$s_i(u_i, Q_i) \longrightarrow s_{i+1}(u_{i+1}, Q_{i+1}), u_{i+1} \in [\mathrm{CTTM}, \mathrm{CPTM}, \mathrm{CRM}, \mathrm{COM}, \mathrm{EBM}, \mathrm{SM}] \tag{9}$$

To facilitate energy-saving, the train often applies the maximum traction force at the $CTTM$ phase like $[s_0, s_1]$ and the appropriate braking force in the SM phase like $[s_{i-1}, s_i]$, in this way the train can reduce the energy consumption, meanwhile adding the coasting condition before the stopping and braking phase can effectively increase the passenger's comfort [22-23].

In summary, the Optimization framework of train operation curve can be illustrated as follows.

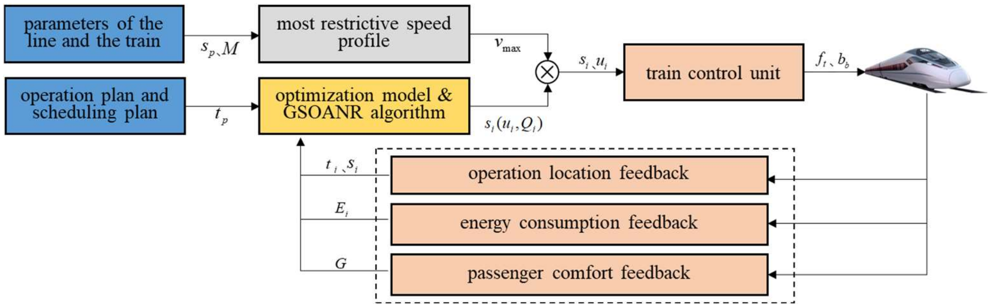

Figure 4. Optimization framework of train operation curve.

3. Optimization methodology based on GSOANR algorithm

Table 2. Symbols of the algorithms.

Symbol	Description
l_0	Initial luciferin value
$l_i(t)$	The luciferin value of individual i at time t
η	Luciferin decay constant ($0 < \eta < 1$)
$Q(x_i(t+1))$	The fitness value of individual i at time $t+1$
γ	Luciferin enhancement constant
$p_{ij}(t)$	Probability of individual i moves towards an individual j
$r_d^i(t+1)$	The neighborhood range of individual i at time $t+1$
n_t	The parameter related to control the number of neighbors
$N_i(t)$	The number of the neighborhood individuals at time t
n	Number of iterations
$\varphi(n)$	The adaptive neighborhood range parameter at nth generation
$MaxGen$	The max generation times
$diversity(n)$	The diversity of the swarm
N	Population size of the swarm
D	The dimensionality of the problem
$x_{ij}(n)$	The jth value of the ith individual firefly

As one of the typical multi-objective optimization problems, the energy consumption reduction problem of trains can also be solved by the intelligence algorithms efficiently. The standard GSO algorithm possesses avoidance of being trapped in local optimum and has fewer parameters which makes it easy to apply to the problems [24]. The traditional intelligent optimization algorithms such as genetic algorithm encounter bottlenecks in the train speed trajectory optimization problem, hence this paper proposes a modified GSO algorithm, namely GSOANR (GSO algorithm with adaptive neighborhood range), to improve the convergence rate and solution precision.

3.1. Standard GSO Algorithm

In standard GSO algorithm, individual fireflies, which contain equal quantity of luciferin l_0 initially, rely on mutual attractions to move around and finally find the solution after iterations. Each iteration is composed of a luciferin update phase and a movement phase which is under the transition rule [24- 26].

Luciferin Update Phase. During the iterations, the luciferin updates of the individuals depend on the fitness value of the individual at the current position and the former luminescence value. The luciferin update rule can be given by **Equation (10)**.

$$l_i(t+1) = (1-\eta)l_i(t) + \gamma Q(x_i(t+1)) \tag{10}$$

Movement Phase. In GSO algorithm, the individual firefly with a larger fitness value has a greater attraction to the other individuals around, and the further away the distance the lower the brightness. The set of neighbors of individual i at time t can be calculated as follows:

$$N_i(t) = \{j: \|x_j(t) - x_i(t)\| < r_d^i(t); l_i(t) < l_j(t)\} \tag{11}$$

Where, $\|x_j(t) - x_i(t)\|$ represents the Euclidean norm of the difference between $x_j(t)$ and $x_i(t)$; $r_d^i(t)$ is the variable neighborhood range associated with individual i at time t. For each individual i, the probability of moving toward a neighbor $j \in N_i(t)$ is given by:

$$p_{ij}(t) = \frac{l_j(t) - l_i(t)}{\sum_{k \in N_i(t)}(l_k(t) - l_i(t))} \tag{12}$$

If the individual i moves towards an individual j with probability $p_{ij}(t)$ given by **Equation (14)**, then the movements can be described as follows, among them $s(>0)$ is the step size.

$$x_i(t+1) = x_i(t) + s\left(\frac{x_j(t) - x_i(t)}{\|x_j(t) - x_i(t)\|}\right) \tag{13}$$

Transition rule. In move phase, the set of neighbors is corresponding with the variable neighborhood range $r_d^i(t)$. The initial neighborhood range of each individual at the beginning is r_0, the rule of updating the neighborhood range of each individual is given as follows.

$$r_d^i(t+1) = \min\{r_i, \max\{0, r_d^i(t) + \varphi(n_t - |N_i(t)|)\}\} \tag{14}$$

where, φ is a constant parameter and n_t is used to limit the number of the neighbors. Eventually more fireflies will move towards the firefly with a larger fitness value.

3.2. GSOANR algorithm

The GSOANR algorithm adopts the definition of the adaptive neighborhood range inspired by the concept of the diversity of the swarm [27]. According to the working phase and transition rule of the standard GSO algorithm, individuals with lower brightness are attracted to individuals with higher brightness and thus move towards them, the equation for neighborhood range update under the effect of attraction is given in **Equation (14)**, among them φ is a constant parameter.

In the proposed GSOANR algorithm, φ is replaced with the diversity of the swarm $\varphi(n)$ as follows.

$$\varphi(n) = 1/\exp(2n/MaxGen) * 1/diversity(n) \quad (15)$$

$$diversity(n) = \frac{1}{N}\sum_{i=1}^{N}\sqrt{\sum_{j=1}^{D}\left(x_{ij}(n) - \overline{x_j(n)}\right)^2} \quad (16)$$

among them, $MaxGen$ is the max generation number, N and D represent the population size of the swarm and the dimensionality of the problem, respectively.

The adaptive neighborhood range parameter φ is composed of two parts: the exponentially decreasing parameter $1/\exp(2n/MaxGen)$ and diversity parameter $1/diversity(n)$. The exponentially decreasing parameter decreases from 1 to 0 as the population iteration proceeds. The diversity parameter is responsible for adjusting the neighborhood range according to the diversity. When the value of the population diversity is low, it implies that the algorithm may have fallen into the local optimum. When the population diversity is high, it means that the algorithm has a strong global exploitation ability, meanwhile it is helpful for avoiding the algorithm to miss the optimal value.

To compare the performance of the GSOANR algorithm with standard GSO algorithm, this paper used 4 benchmark functions as listed in **Table 3**, among them f_1 and f_2 are single-mode functions and the others are multi-mode functions [28-29].

Table 3. Test functions.

	Name	Function	Search range	Global optimum
f_1	Sphere	$f_1(x) = \sum_{i=1}^{D} x_i$	[-100,100]	0
f_2	Rosenbrock	$f_2(x) = \sum_{i=1}^{D} [100(x_{i+1} - x_i^2)^2 + (1 - x_i^2)^2]$	[-30,30]	0
f_3	Schwefel 2.26	$f_3(x) = \sum_{i=1}^{D} -x_i sin\sqrt{\lvert x_i \rvert}$	[-500,500]	-418.98*D
f_4	Rastrigin	$f_4(x) = \sum_{i=1}^{D} (x_i^2 - 10cos2\pi x_i + 10)$	[-5.12,5.12]	0

Table 4. Comparison results of 2 algorithms on benchmark test functions.

Function	Algorithm	Best value	Worst value	Mean value	Standard deviation
f_1	GSOANR	**9.17E-02**	**1.33E+02**	**1.09E+01**	**2.36E+01**
	GSO	2.30E-01	1.64E+02	2.12E+01	3.89E+01
f_2	GSOANR	**4.67E-07**	**1.97E-01**	**2.75E-02**	**4.36E-02**
	GSO	7.38E-07	2.30E-01	3.27E-02	5.45E-02
f_3	GSOANR	-4.19E+02	-3.00E+02	**-3.99E+02**	**3.14E+01**
	GSO	-4.19E+02	-3.00E+02	-3.97E+02	3.58E+01
f_4	GSOANR	**4.91E-02**	**2.07E+01**	**6.37E+00**	**4.52E+00**
	GSO	7.12E-01	2.18E+01	6.44E+00	5.53E+00

Table 4 shows the optimization results of the GSO algorithm and the GSOANR algorithm. It is evident that the average value and standard deviation of the results produced by the GSOANR algorithm are better than the results obtained from the GSO algorithm in optimizing all functions.

3.3. Implementation procedure

Design of individuals in the population. To solve the train operation trajectory optimization problem, each individual firefly x_i should represent a feasible train operation strategy, which consists of the driving condition sequence $\{u_i\}$ and the corresponding changeover points $\{s_i\}$, hence defining $x_i = \{u_i, s_i\}$ as the individual firefly, and the population initialization needs to satisfy **Equation (7)**.

Fitness function. Each individual firefly relies on its brightness to attract the other individuals to shift their positions during the process of searching for better solutions. The fitness function which is related to the brightness is defined as the inverse of the cost function defined in **Equation (17)**.

$$Q = \frac{1}{J} = \frac{1}{k_1 \sum_{i=1}^{n} E_i + k_2 \left| t_p - \sum_{i=1}^{n} t_i \right| + k_3 \left| s_p - \sum_{i=1}^{n} s_i \right| + k_4 max\{G\}} \tag{17}$$

Update of operation sequence. As mentioned earlier, each individual firefly in GSO algorithm represents an operation trajectory, which can be descripted as a sequence of operating conditions and transition points, i.e., $x_i = \{u_i, s_i\}$, where $\{u_i\}$ denotes the union of operating conditions in the operation sequence and S denotes the union of the transition points. The update of individual fireflies includes the update of the operating condition sequence, i.e., $x_i(n+1) = \{u_i\,(n), s_i\,(n)\}$ or $\{u_i\,(n), s_j(n)\}$, and the selection is based on the fitness value of the two solutions.

In general, the key steps of the algorithm for optimizing the driving strategies are as follows.

Algorithm 1. Optimization method based on GSOANR algorithm

Randomly initialize N fireflies according to Equation (7) as the initial population;
Calculate the fitness value of each individual firefly x_i according to Equation (17);
t=0;
while (t< MaxGen) **do**
    Update the neighborhood range parameter φ according to Equation (15);
    for i=1: n (all n fireflies) **do**
        for j=1: n (all n fireflies) **do**
            if $Q(x_j) > Q(x_i)$ **then**
                Calculate the probability of moving according to Equation (12);
                Move individual x_i towards x_j according to Equation (13);
                Calculate the fitness value of the new solution x_i according to Equation (17);
            end
        end
    end
    t=t+1;
end

The parameters in GSOANR algorithm that need to be pre-set include the fluorophore volatilization coefficients and the initial population size. According to Huang et al., Kaipa & Ghose, Kim K and other related tests [31-33], the key parameters in the GSOANR and the GSO algorithm are set as listed in **Table 5**, the population size is set to 30, and the maximum number of iterations is 200.

Table 5. Setting of key parameters in the GSOANR and the GSO algorithm.

Parameter	Description	Parameter Value
η	Decay constant of fluorescein	0.40

γ	Fluorescein growth coefficient of the GSO algorithm	0.60
β	The variation coefficient of perceptual radius of the GSO algorithm	0.08
l_0	Luciferin value at the beginning	5

The index coefficient k_i presents the importance of each index in the algorithm, and the value of k_i can be determined by the practical requirements and can be adjusted flexibly under different scenarios. The simulation results of the driving strategies obtained by different methods with different values of k_i are showed in **Figure 5**. Each of the three sets of results corresponds to one of the three typical strategies mentioned in Section 2 respectively.

In group 1, $k_1 = 0.1, k_2 = 0.6, k_3 = 0.2, k_4 = 0.1$; in group 2, $k_1 = 0.35$, $k_2 = 0.35$, $k_3 = 0.2$, $k_4 = 0.1$; and in group 2, $k_1 = 0.6, k_2 = 0.1, k_3 = 0.2, k_4 = 0.1$. Compared with the group 1 and group 2, the group 3 which is corresponding to the integrated optimization strategy has a stable performance in terms of fitness values, meanwhile the consumption of the time and energy are also acceptable. To balance the importance of energy consumption and travel time while taking the other indexes into consideration, the weighting k_1 for the energy performance measure is set as 0.35, for the time performance measure the weighting k_2 is also set to be 0.35, for the stopping position performance measure k_3 is 0.20, and the comfort measure weighting k_4 is 0.10.

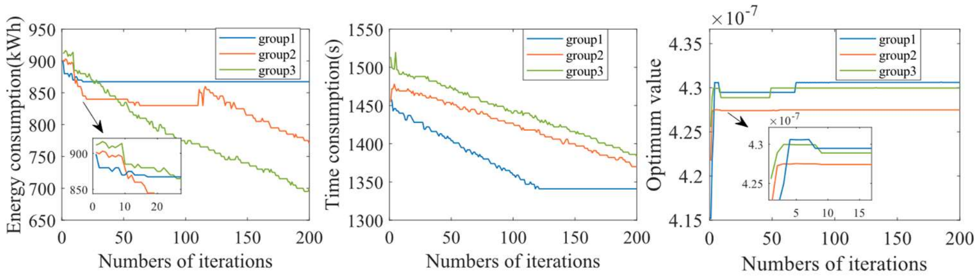

(a) (b) (c)

Figure 5. The process of iteration with different values of k_i. (a) the energy consumption of iterations with different values of k_i, (b) the time consumptions of iterations with different values of k_i, (c) the optimum value of iterations with different values of k_i.

4. Simulation and analysis

To confirm the efficacy of the proposed optimization method, this section executes two cases in which the major difference is the optimization method for generating the operation trajectory while the other parameters like the type of the train and the line parameters are all the same. Case 1 compares the traditional GSO algorithm with the GSOANR algorithm for train trajectory optimization. And case 2 compares the GSOANR based train trajectory optimization with an existing optimization method which is based on Q-learning algorithm.

4.1. Case 1

This case adopts the CR400BF type high-speed train which is composed of 4 trailers cars and 4 motor cars and uses a real line data between Heishan North Station and Fuxin Station for simulation. The real line in simulation is chosen from Beijing-Shenzhen Line referencing from the paper of [11]. **Table 6** gives some details of the line and the train.

Table 6. The parameters of the line and the train.

Parameter	Description	Parameter Value
s_p	Length of the line	58 km
t_p	Planned travel time	23 min
v_{max}	Speed limitation for the whole road	288 km/h
M	The mass of the train	913 t
$w_0(v)$	Basic resistance of the train	$0.399 + 0.0013 \cdot v + 0.000109 \cdot v^2 \ \ N/kN$
$f_t(v)$	Train motoring characteristics	$\begin{cases} 267 - 0.243 \cdot v \ \ kN \ \ (0 \le v < 160\ km/h) \\ 0.0021v^2 - 1.7308 \cdot v + 446.75\ kN \ \ (v \ge 160\ km/h) \end{cases}$
$b_b(v)$	Train braking characteristics	$\begin{cases} 280 \cdot v/10 \quad kN \quad (0 \le v < 10\ km/h) \\ -0.2241v + 281.74 \quad kN \quad (10 \le v < 200\ km/h) \\ 0.0017v^2 - 1.5602v + 475.38\ kN \ \ (v \ge 200\ km/h) \end{cases}$

The operation trajectory generated by the traditional GSO algorithm is analyzed first. In the algorithm, the population size is 30, the maximum number of iterations is 200, the decay constant of fluorescein is set to 0.40, the fluorescein growth coefficient and the variation coefficient of perceptual radius are set to 0.60 and 0.08 respectively. The program randomly generated 30 train operation trajectories, and each firefly corresponds to one trajectory which changes its location based on the comparison of the fitness valve to the individuals in the range. After iterations most of the fireflies converge to the optimal one.

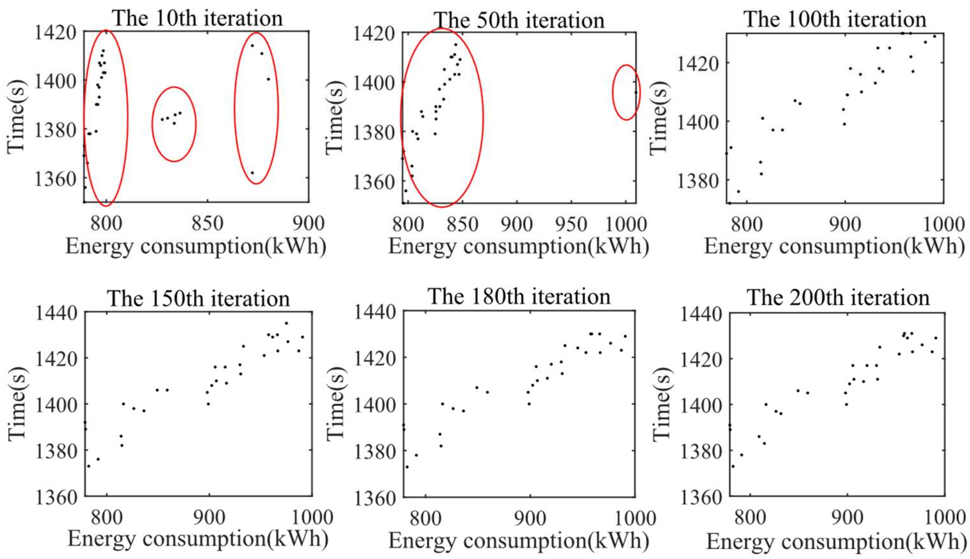

Figure 6. Distribution of each individual in different iterations of the standard GSO algorithm.

Figure 6 shows the solutions of the 10th, 50th, 100th, 150th, 180th and 200th generations, from which we can observe that when the evolution starts, fireflies closer to each other are more easily to gather around, at this stage, the distance between individuals has a bigger influence, that is the reason of the clusters of individual fireflies as the red circle noted. Finally, the energy consumption sums up to 765.023 kWh and the running time is 1371 s.

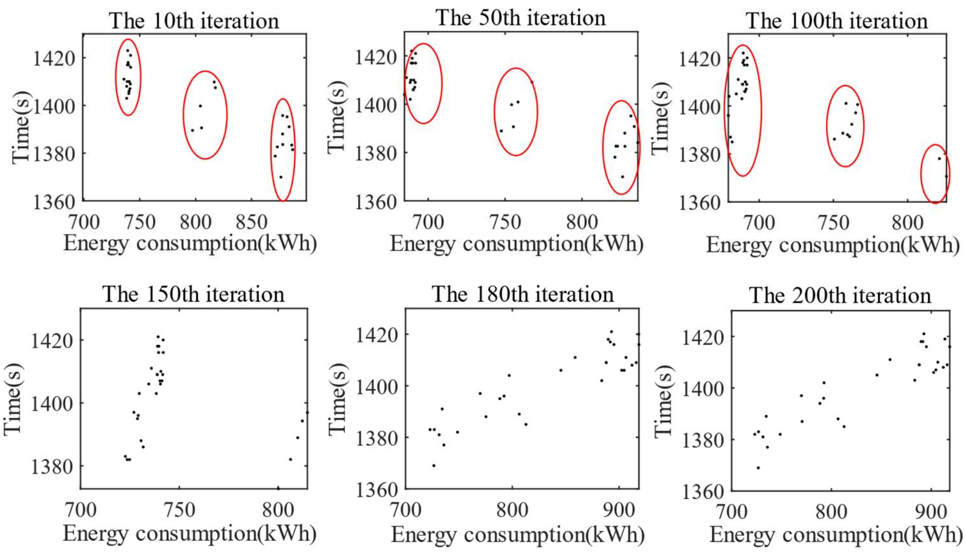

Figure 7. Distribution of each individual in different iterations of the GSOANR algorithm.

Then the optimization method based on the GSOANR algorithm is used to generate the optimal trajectory, whose solutions of the 10th, 50th, 100th, 150th, 180th and 200th generations are shown in **Figure 7**. In the whole iteration process, the individuals of each generation aim at searching the optimal trajectory which has the lowest fitness value. There are two distinctive features: one is that the energy consumption of the entire population ranges from 700 to 900 kWh, where fireflies with too little energy consumption generally appear to stop too early and their stopping position indexes are large, resulting low fitness values; On the other hand, fireflies with too much energy consumption also have low fitness values due to long running time.

Figure 8 illustrates the optimal trajectories generated by the standard GSO algorithm and the GSOANR algorithm, and the comparison data of the optimal solutions are listed in **Table 7**. The most significant difference between the standard algorithm and the improved algorithm is the definition of the neighborhood range parameter. It's not hard to find that, while GSOANR algorithm has greater search capabilities hence the individuals can search better trajectory, and the train runs at constant traction mode on short-distance tracks and switches to the cruising mode when the speed is reaching the limit on straight long-distance tracks. The energy consumption of the improved algorithm is 722.449 kWh and reduces by 5.6% than that of the standard algorithm. According to the analysis and comparison of two optimization method, the trajectory generated by the standard GSO algorithm is a desirable operation trajectory in practice, while the GSOANR algorithm is further more compliant with energy efficiency.

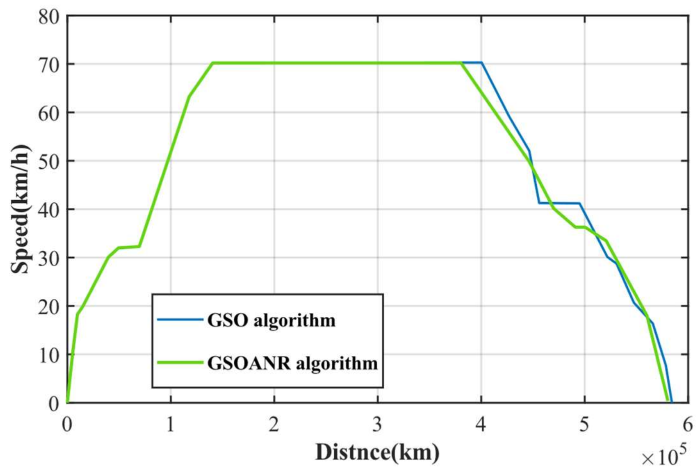

Figure 8. The optimal trajectories by the standard GSO algorithm and the GSOANR algorithm.

Table 7. The comparison data of the optimal solutions by GSO and GSOANR algorithms.

Optimization methods	Energy consumption (kWh)	Planned running time (s)	Running time (s)
GSO Algorithm	765.023	1370	1371
GSOANR Algorithm	**722.449**	1370	1372

4.2. Case 2

In this case, the comparison with the optimization method based on the GSOANR algorithm and the Q-learning algorithm [11] is made. These two methods are different in the ways of algorithm improvement and trajectory coding.

In [11], the railway line between Heishan North Station and Fuxin Station is simulated. The operation distance is 58 km and the planned travel time is 23 min. As the final simulation results show, the energy consumption of the Q-learning Algorithm which is trained for 6×10^6 times is 886.261 kWh, and the energy consumption of which is trained for 1×10^7 times is 922.367 kWh. The increase in the number of training sessions resulted in a further improvement in train punctuality, with a reduction in running time of 8 s, but an increase in energy consumption of only 4%.

To make a comparison of these two different methods, the operation trajectory should be optimized under the same conditions of both the train and the line, **Figure 9** shows the optimal trajectories generated by those two different methods, respectively. It's noted that these trajectories are similar at the beginning, and the trajectory generated by the GSOANR algorithm is more prefer to use coasting mode when approaching stations, which can reduce the energy consumption because the traction power is zero under the coasting mode. Besides, the energy feedback of the braking mode also reduces the consumption of the energy. The comparison data are also given in **Table 8**. As the result shows, the energy consumption of the GSOANR algorithm is 722.449 kWh, reduces by 19.5%. Hence, the energy efficiency of the GSOANR algorithm based optimization method is confirmed again.

Table 8. The comparison data of the optimal solutions by different approaches.

Optimization methods	Energy consumption (kWh)	Planned running time (s)	Running time (s)
Q-learning Algorithm (1*10^7)	922.367	1370	1369
Q-learning Algorithm (6*10^6)	886.261	1370	1377
GSOANR Algorithm	**722.449**	1370	1372

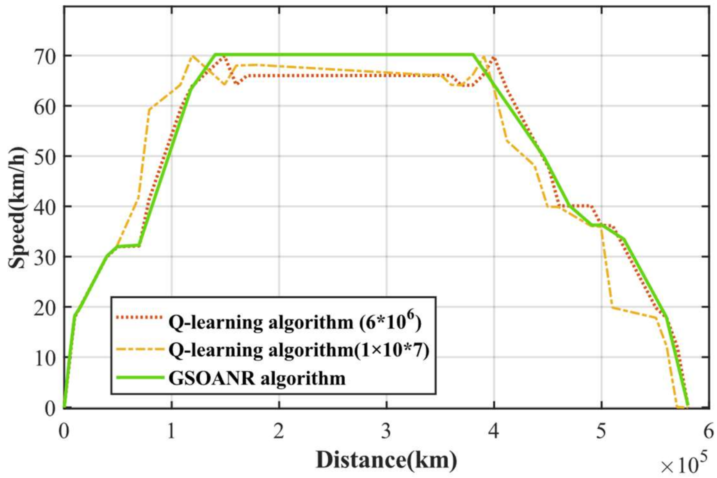

Figure 9. The optimal trajectories by algorithms. (a) Q-learning algorithm and the GSOANR algorithm, (b) the standard GSO algorithm and the GSOANR algorithm.

5. Discussion and conclusion

As traditional diesel trains are expected to be replaced by hybrid and fully electrified trains in the next decades [33], the electricity demand of the railway sector will increase dramatically, which will inevitably impose great pressure on future power grids largely running on renewable energies. Hence it is important to reduce the electricity demand by optimizing the train trajectory. However, the train trajectory optimization needs to consider multiple criterions and constraints, and the ATO system is not mature enough for energy-saving compared with the experienced drivers. Hence it is challenging to formulate and solve the optimization problem.

The main contributions of this paper include:1) developed a multi-objective optimization framework for operation trajectory optimization of the train by considering the new features of ATO systems introduced in electrified and high-speed trains; 2) proposing six quantitative energy-saving performance measures and leading to the establishment of the multi-objective optimization model; 3) a modified GSO algorithm namely GSOANR is used to search for the optimal operation trajectory. The proposed method has been verified trajectory planning for a 58km long route between the Stations of the Beijing-Shenzhen Passenger Line in China, and has achieved about 19.5% and about 5.6% energy reduction than the Q-learning algorithm and the standard GSO algorithm respectively, which proves that the method of this paper is informative for the study of train trajectory optimization.

Funding

This work was supported by the Special Funding Project for Innovation-driven Development of Guangxi

Providence (2016YFB1200602-34); the Natural Science Foundation of Hunan Province of China (2021JJ30828).

References

[1] Scheepmaker GM, Goverde R, Kroon LG. Review of energy-efficient train control and timetabling. Eur J Oper Res. 2017;257(2017):355–376.
[2] Yin JT, Tang T, Yang LX, et al. Research and development of automatic train operation for railway transportation systems: A survey. Transp Res Part C Emerging Technol. 2017; 85:548-572.
[3] Li W, Zhong Q, Peng Q, et al. Metro train delay-recovery strategy considering passenger waiting time and energy consumption: A real-world case study. Int J Rail Transp. 2022; 1–26.
[4] Hu YL, Ling L, Wang KY. An analytical method for train dynamic behavior on long steep grades of high-speed railway [in Chinese]. J Southwest Jiaotong Univ, 2022, 57(2): 277-285.
[5] Spiryagin M, Wu Q, Wolfs P, et al. Comparison of locomotive energy storage systems for heavy-haul operation. Int J Rail Transp. 2018;6(1):1-15.
[6] Albrecht A, Howlett P, Pudney P, et al. The key principles of optimal train control—Part 1: Formulation of the model, strategies of optimal type, evolutionary lines, location of optimal switching points. Transp Res Part B Methodol. 2016; 94: 482-508.
[7] Albrecht A, Howlett P, Pudney P, et al. The key principles of optimal train control—Part 2: Existence of an optimal strategy, the local energy minimization principle, uniqueness, computational techniques. Transp Res Part B Methodol. 2016;94: 509-538.
[8] Bai Y, Ho TK, Mao BH, et al. Energy-Efficient Locomotive Operation for Chinese Mainline Railways by Fuzzy Predictive Control. IEEE Trans Intell Transp Syst. 2014;15(3):938-948.
[9] Zhou LS, Tong L, Chen JH, et al. Joint optimization of high-speed train timetables and speed profiles: A unified modeling approach using space-time-speed grid networks. Transp Res Part B Methodol. 2017;97:157-181.
[10] Liu SQ, Cao F, Xun J, et al, authors. IEEE 18th International Conference on Intelligent Transportation Systems; 2015 Sep 15-18; Las Palmas de Gran Canaria, Spanish.
[11] Zhang M, Zhang Q, Zhang ZX. A Study on Energy-saving Optimization for High-Speed Railways Train based on Q-learning Algorithm [in Chinese]. Rail Transp Econ. 2019;41(12):111-117.
[12] Wang C, Liu W, Tian Q, et al, authors. 2020 IEEE 23rd International Conference on Intelligent Transportation Systems;2020 Sep 20-23; Rhodes, Greece.
[13] Keskin K, Karamancioglu A, authors. IEEE International Conference on Intelligent Systems; 2016 Sep 4-6; Sofia and Varna, Bulgaria.
[14] Song Y, Song W. A novel dual speed-curve optimization based approach for energy-saving operation of high-speed trains. IEEE Trans Intell Transp Syst. 2016;17(6): 1564-1575.
[15] Wang X, Tang T, Su S, et al. An integrated energy-efficient train operation approach based on the space-time-speed network methodology. Transp Res Part E Logist Transp Rev. 2021;150: 102323.
[16] Cheng JF, Feng K, Li K. CTCS3+ATO High Speed Railway Train Control Technology [in Chinese]. China Rail. 2019;01:74-77.
[17] Li W, Zhao SZ, Li K, authors. 2021 International Conference on Life System Modeling and Simulation & 2021 International Conference on Intelligent Computing for Sustainable Energy and Environment; 2021 Oct 30- Nov 1; Hangzhou, China.
[18] Shi C, Zhao C, Zhang X, et al. Coupled discrete-continuum approach for railway ballast track and subgrade macro-meso analysis. Int J Pavement Eng. 2021;22(13):1744-1759.
[19] Zhu L, Lei C, Roberts C, et al. Dynamic Trajectory Optimization Design for Railway Driver Advisory System. IEEE Intell Transp Syst Mag. 2018;10(1):121-132.
[20] Song Y, Song W. A novel dual speed-curve optimization based approach for energy-saving operation of high-speed trains. IEEE Trans Intell Transp Syst. 2016;17(6):1564-1575.
[21] Sun ZK, Wang TT, Wu F. Numerical investigation of influence of pantograph parameters and train length on aerodynamic drag of high-speed train. J Cent South Univ. 2020;27(04):1334-1350.
[22] Su S, Tang T, Li X. Driving strategy optimization for trains in subway systems. Proc Inst Mech Eng, Part F:J Rail Rapid Transit. 2018;232(2): 369-383.
[23] Scheepmaker GM, Pudney PJ, Albrecht AR, et al. Optimal running time supplement distribution in train schedules for energy-efficient train control. J Rail Transp Plann Manage. 2020;100180.
[24] Krishnanand KN, Ghose D, Prasad B. Glowworm swarm based optimization algorithm for multimodal functions with collective robotics applications. Multiagent Grid Syst. 2006; 2(3):209-222.
[25] Abualigah L. Group search optimizer: a nature-inspired meta-heuristic optimization algorithm with

its results, variants, and applications. Neural Comput Appl. 2020; 33(7): 2949-2972.
[26] Reddy D L, Puttamadappa C, Suresh H N. Merged glowworm swarm with ant colony optimization for energy efficient clustering and routing in wireless sensor network. Pervasive Mob Comput. 2021;71:101338.
[27] Chowdhury A, De D. FIS-RGSO: dynamic fuzzy inference system based reverse glowworm swarm optimization of energy and coverage in green mobile wireless sensor networks. Comput Commun. 2020;163:12-34.
[28] Brest J, Greiner S, Boskovic B, et al. Self-adapting control parameters in differential evolution: A comparative study on numerical benchmark problems. IEEE Trans Evol Comput. 2006;10(6): 646-657.
[29] Xin Y, Yong L. Evolutionary programming made faster. IEEE Trans Evol Comput. 1999;3(2):82-102.
[30] Huang Z, Zhou Y. Using Glowworm Swarm Optimization Algorithm for Clustering Analysis. J Convergence Info Tech. 2011;6(2):78-85.
[31] Kaipa KN, Ghose D. Glowworm swarm optimization: algorithm development. Cham: Springer; 2017.
[32] Kim K, Chien IJ. Simulation-Based Analysis of Train Controls under Various Track Alignments. J Transp Eng. 2010;136(11):937-948.
[33] Din T, Tian ZB, Li K, et al. Operation and Energy Evaluation of Diesel and Hybrid Trains with Smart Switching Controls. J Transp Eng. 2021;116(1).